



Spectral sensitivity of ALOS, ASTER, IKONOS, LANDSAT and SPOT satellite imagery intended for the detection of archaeological crop marks

Athos Agapiou, Dimitrios D. Alexakis & Diofantos G. Hadjimitsis

To cite this article: Athos Agapiou, Dimitrios D. Alexakis & Diofantos G. Hadjimitsis (2014) Spectral sensitivity of ALOS, ASTER, IKONOS, LANDSAT and SPOT satellite imagery intended for the detection of archaeological crop marks, International Journal of Digital Earth, 7:5, 351-372, DOI: [10.1080/17538947.2012.674159](https://doi.org/10.1080/17538947.2012.674159)

To link to this article: <https://doi.org/10.1080/17538947.2012.674159>



Published online: 04 Apr 2012.



Submit your article to this journal [↗](#)



Article views: 1079



View related articles [↗](#)



View Crossmark data [↗](#)



Citing articles: 6 View citing articles [↗](#)

Spectral sensitivity of ALOS, ASTER, IKONOS, LANDSAT and SPOT satellite imagery intended for the detection of archaeological crop marks

Athos Agapiou*, Dimitrios D. Alexakis and Diofantos G. Hadjimitsis

Department of Civil Engineering and Geomatics, Cyprus University of Technology, Limassol, Cyprus

(Received 13 November 2011; final version received 6 March 2012)

This study compares the spectral sensitivity of remotely sensed satellite images, used for the detection of archaeological remains. This comparison was based on the relative spectral response (RSR) Filters of each sensor. Spectral signatures profiles were obtained using the GER-1500 field spectroradiometer under clear sky conditions for eight different targets. These field spectral signature curves were simulated to ALOS, ASTER, IKONOS, Landsat 7-ETM+, Landsat 4-TM, Landsat 5-TM and SPOT 5. Red and near infrared (NIR) bandwidth reflectance were re-calculated to each one of these sensors using appropriate RSR Filters. Moreover, the normalised difference vegetation index (NDVI) and simple ratio (SR) vegetation profiles were analysed in order to evaluate their sensitivity to sensors spectral filters. The results have shown that IKONOS RSR filters can better distinguish buried archaeological remains as a result of difference in healthy and stress vegetation (approximately 1–8% difference in reflectance of the red and NIR band and nearly 0.07 to the NDVI profile). In comparison, all the other sensors showed similar results and sensitivities. This difference of IKONOS sensor might be a result of its spectral characteristics (bandwidths and RSR filters) since they are different from the rest of sensors compared in this study.

Keywords: RSR filters; spectral sensitivity; archaeological remains; crop mark detection; spectroscopy

1. Introduction

1.1. Crop marks

Vegetation crop marks may be formed in areas where vegetation overlay near-surface archaeological remains. These features retain soil moisture with different percentage of moisture compared to the rest of the crops of an area. Depending of the type of feature, crop vigour may be enhanced or reduced by buried archaeological features (Winton and Horne 2010).

For instance, if vegetation grows above buried ditches or moat, then the crop growth is likely to be enhanced. This is due to the topsoil which holds more moisture than in the surrounding context (especially during periods when water stress develops). This phenomenon can be recorded from any airborne and spaceborne platform and is referred to as a positive crop mark (Stanjek and Fabinder 1995,

*Corresponding author. Email: athos.agapiou@cut.ac.cy

Sharpe 2004, Jonson 2006, Lasaponara and Masini 2007). However, in cases where there is not enough moisture in the retentive soil and there is lack of available water for evapotranspiration (e.g. vegetation grown above building remains or compacted ground), the developed marks are characterised as negative crop marks. These are less common than the positive ones (Riley 1979, Sharpe 2004, Jonson 2006, Lasaponara and Masini 2007). Comparing the two different kinds of marks, the positives are normally taller with darker green and healthy foliage than the negative crop marks. On the other hand, the negative crop marks tend to be paler green with lighter coloured appearance when monitored from the air (Sharpe 2004, Jonson 2006).

Furthermore, recent studies argue that there are many complex factors involved in the capturing of crop marks. Several researches (Mills and Palmer 2007, Winton and Horne 2010), have found that the evolution of crop mark can be a combination of different factors and parameters such as moisture availability, the availability of dissolved nutrients to the crops (at crucial growing times and periods for the plant), the crop, the soil type itself and finally the soil depth.

For example, Sharpe (2004) argues that archaeological crop marks in England are recorded in cereal crops especially during warm and dry summer months while Ciminale *et al.* (2009) mentions that for the Mediterranean region, crop marks are better visible from the beginning of spring up to the half or end of May.

1.2. Remote sensing in archaeology

Several researchers, over the last decades, showed that multispectral images can be used in different archaeological environments in order to detect subsurface remains (Bewley 2003, Altaweel 2005, Beck 2007, Alexakis *et al.* 2009, 2011) or even to monitor archaeological sites (Agapiou and Hadjimitsis 2011; Hadjimitsis *et al.* 2011, 2009). Bewley (2003) reported that more than 50% of all known archaeological sites in the UK were revealed from airborne platforms. Both high and very high resolution satellite sensors give the opportunity to examine and study crop marks related to sub-surfaces anomalies, using different spectral and spatial characteristics (Lasaponara and Masini 2001, Parcak 2009). For example, very high resolution satellite imagery (< 4 m spatial resolution) such as IKONOS and QuickBird have been used in the past for the detection of archaeological remains based on vegetation marks as shown by Lasaponara and Masini (2005, 2006, 2007) and Altaweel (2005). Masini and Lasaponara (2007) used multispectral Quickbird images for the detection of archaeological remains in Italy. Beck (2007) used IKONOS satellite images for the case of Homs in Syria, while Laet *et al.* (2007) have extracted archaeological features using the same satellite sensor for a case study in Turkey. In addition to the aforementioned, data based on low spectral and spatial resolution imagery has also been used from Clark *et al.* (1998), Sarris and Jones (2000) and Tripathi (2000).

Although very high imagery data-set provide many advantages to researchers compared to high resolution imagery (< 30 m spatial resolution), sometimes the high cost can be prohibitive to be used for archaeological research. Indeed, multispectral high resolution satellite imagery has been used for the detection of sub-surface archaeological remains in many case studies. Altaweel (2005) has employed ASTER satellite images in the archaeological context of Mesopotamia. Alexakis *et al.* (2009, 2011) used both high and very high resolution satellite images

(ASTER, Landsat TM and IKONOS) for the detection of archaeological remains in the Thessalian plain in Greece. Finally, Agapiou and Hadjimitsis (2011) used freely distributed Landsat TM/ETM+ satellite imagery and ground spectroradiometric measurements for monitoring phenological cycle of barley crops over the archaeological area of Palaepaphos, in Cyprus.

1.3. Ground spectroscopy

Field spectroradiometric measurements have been used in many of remote sensing applications including, vegetation canopy reflectance modelling, spectral mixture analysis, classification techniques and predictive modelling (Peddle *et al.* 2001). Field spectroradiometers may be used in order to record the reflectance amount of crops over archaeological areas as shown by Agapiou *et al.* (2010, 2012) and Agapiou and Hadjimitsis (2011). Spectroradiometers can measure the amount of energy (radiance) reflected from a ground area (e.g. crops) and then converted to reflectance using calibration panels (Peddle *et al.* 2001).

Field spectroradiometers can be used to give calibrated measurements since such instruments are often accompanied by calibrated Lambertian surface panel. Milton *et al.* (2009) emphasises that a critical factor for reliable results is the calibration of the panel. Indeed, as Milton and Rollin (2006) mentioned, in cases where ‘single-beam’ measurements are taken within one minute, the radiation is actually unchanged. The radiation is also affected by the zenith angle of the sun and the coordinates of the area of interest (Milton 1987). One way to eliminate these errors is to measure the before and after of the special calibration target. This may be true in most cases but in the presence of cloud cover or a sudden change of the weather this can be incorrect (see Milton 1987). Such considerations have been already taken into account for the purpose of this study.

1.4. Spectral sensitivity of satellite sensors

Chander *et al.* (2009) mentioned that the detection and quantification of change (e.g. crop marks) in the earth’s environment, depends on the satellite’s characteristics (mainly spectral and spatial). Teillet *et al.* (2007) highlighted that data from the various imaging sensor systems must be on a consistent radiometric calibration scale and hence, sensor radiometric calibration is of critical importance. The methods and measurements involved in sensor radiometric calibration can be grouped into three domains (Teillet *et al.* 2007):

- on the ground prior to launch, onboard the spacecraft post-launch, including reference to lamp sources and/or solar illumination (e.g. Markham *et al.* 1997) or
- lunar illumination using radiative codes to simulate Top of Atmosphere signal (e.g. Trishchenko *et al.* 2002) and
- approaches using earth scenes images captured in-flight (e.g. Teillet *et al.* 2007).

However, as Trishchenko *et al.* (2002) stated, the total relative uncertainties of calibration are within 5% for satellite sensors. Although spectral uncertainties have been examined elsewhere (Trishchenko *et al.* 2002, Teillet *et al.* 2007, Trishchenko

2009), there is a lack of literature regarding the different spectral profiles provided from multispectral satellite sensors used for the detection of sub-surfaces anomalies. The detection of buried archaeological remains is based mostly on examining the response of Red and near infrared (NIR) part of spectrum and the use of vegetation indices (such as normalised difference vegetation index [NDVI] and simple ratio [SR]).

Further, such spectral uncertainties satellite images need to be atmospherically and geometrically corrected, before being subjected to any post-processing techniques (Agapiou *et al.* 2011a, Lillesand *et al.* 2004). Other corrections that must be taken into account are, sun elevation, elevation of the area of interest, etc. (Campbell 2002).

The overall aim of this study is to examine the spectral characteristics of seven different satellite sensors using field spectroradiometric data (spectral signatures profiles) derived from different field campaigns over a 'test field' simulating an archaeological environment. This study does not intend to study the calibration procedures of each sensor itself but to evaluate the sensitivity of these sensors in the context of crop marks detection. Finally, in this study vegetation indices were used to illustrate the potential of each sensor for detecting subsurface archaeological remains.

The direct comparison of reflectance measurements acquired from fine resolution sensors such as field spectroradiometers with other sensors of very high or high resolution such as those mentioned in this study, has been discussed by other researchers (Curran and Williamson 1986, Milton *et al.* 2009, Wu and Liang Li 2009). Indeed, different scaling techniques (i.e. transfer of data content from one scale to another one) have been extensively reported by Malenovsky *et al.* (2007). The bottom-up approach, up-scales information from smaller to larger observational scales (e.g. from spectroradiometer to high resolution pixel size). Nevertheless, Jarvis (1995) mentions that scaling represents a scientific challenge, due to the non-linear nature between processes and variables, and heterogeneity of characteristics determining the rates of processes. Nevertheless, many researches apply simple models in order to evaluate scale differences (Marceau *et al.* 1994, Tran *et al.* 2011)

The choice of the resampling algorithm was based on the following considerations. The goal of the study is not to simulate all conditions involved in data acquisition using satellite sensors, but to investigate the spectral sensitivity of the sensors. Therefore, a simple model can be used, taking into consideration the relative response filters of each sensor. Such approach has also been presented for vegetation studies by Papadavid *et al.* (2011) and Agapiou and Hadjimitsis (2011).

2. Sensors overview

2.1. General characteristics

This study included the evaluation of both high and very high resolution multispectral satellite sensors. Satellite images acquired from these sensors are used for the detection of archaeological remains using mainly the red and NIR part of spectrum. Table 1 indicates the spectral and spatial characteristics of the satellites sensors used in this study (ALOS-AVNIR-2, EO-ASTER, IKONOS, Landsat 4 and 5 TM/ 7 ETM+ and SPOT 5 -HRV):

Table 1. Satellite characteristics used in this study.

Satellite sensor	Spectral resolution		Spatial resolution	
	Bands	Wavelength		
ALOS-AVNIR-2	1	Blue	0.42–0.50 (μm)	10 m
	2	Green	0.52–0.60 (μm)	
	3	Red	0.61–0.69 (μm)	
	4	NIR	0.76–0.89 (μm)	
EO-ASTER	1	Green	0.52–0.60 (μm)	15 m
	2	Red	0.63–0.69 (μm)	
	3	NIR	0.76–0.86 (μm)	
IKONOS	1	Blue	0.445–0.516 (μm)	4 m
	2	Green	0.506–0.595 (μm)	
	3	Red	0.632–0.698 (μm)	
	4	NIR	0.757–0.853 (μm)	
Landsat 4 TM	1	Blue	0.45–0.52 (μm)	30 m
Landsat 5 TM	2	Green	0.52–0.60 (μm)	
Landsat 7 ETM +	3	Red	0.63–0.69 (μm)	
	4	NIR	0.75–0.90 (μm)	
SPOT 5 -HRV	1	green	0.50–0.59 (μm)	10 m
	2	red	0.61–0.68 (μm)	
	3	NIR	0.78–0.89 (μm)	

NIR, near infrared.

Figure 1 shows the spectral bandwidth of the sensors, mentioned in this study, compared to a typical spectral signature of vegetation. It is interesting to note the bandwidth of the sensors especially for the NIR bands: IKONOS sensor has a bandwidth of approximately $0.096 \mu\text{m}$ in contrast to $0.100\text{--}0.150 \mu\text{m}$ of the other sensors. However, as it is indicated, all sensors have similar but not identical spectral resolutions (except from the Landsat sensors).

This observation has prompted to investigate, if the capability of the sensor to ‘capture’ information regarding vegetation might affect the interpretation results regarding crop marks, over archaeological areas using vegetation indices.

Even though spatial resolution has not been examined in this study, it is also a key parameter for the detection or not of buried archaeological remains due to the fact that the use of high spatial resolution images, at a resolution close to the actual spatial pattern of remains, reduces the possibility of the impact of mixed pixels (Rowlands and Sarris 2007).

2.2. Relative spectral response (RSR) filters

Trishchenko *et al.* (2002) have mentioned that the total relative uncertainties of calibration are within 5% for satellite sensors. An essential part of this uncertainty is related to the effect of RSR filters which describes the relative sensitivity of sensors to energy of different wavelength. These filters have a value of 0–1 and have no units since they are relative to the peak response. They describe the instrument’s relative sensitivity to radiance at various part of the electromagnetic spectrum (Wu *et al.* 2010).

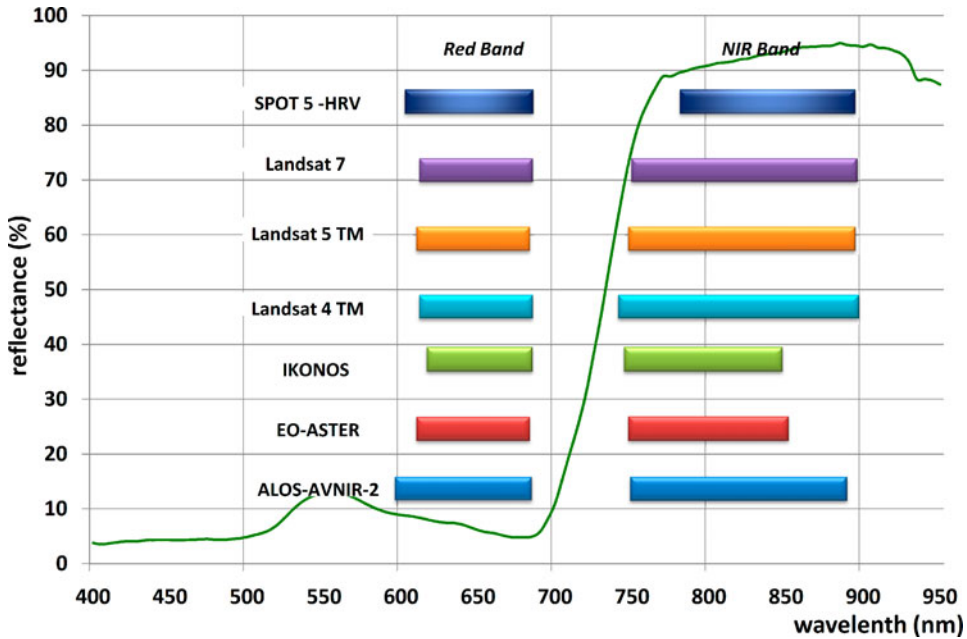


Figure 1. Red and NIR bandwidths of the different sensors mentioned in this study in comparison with a typical vegetation spectral profile.

Such kinds of filters are used for any satellite or aerial sensor. For example, in Landsat 5 TM, each reflective band is sensed by an array of 16 detectors and the signal from an individual detector is referred to as a channel. Although there are multiple detectors per band, there is only one filter (Markham and Barker 1985). The use of such filters is, to produce individual colour, utilising the filters on the sensors, to subdivide the light received into wavelength intervals (the bands).

Bandpass filters are used in the same way in spectroradiometers in order to transmit a certain wavelength band and block others. The reflectance from the spectroradiometer was calculated based on the wavelength of each sensor and the RSR filter as follows:

$$R_{band_i} = \frac{\sum (R_i * RSR_i)}{\sum RSR_i} \tag{1}$$

Where: R_{band_i} = reflectance at a range of wavelength (e.g. Band 1); R_i = reflectance at a specific wavelength (e.g. R 0.450 μ m); RSR_i = relative response value at the specific wavelength.

Figure 2 shows the RSR filters diagrams for ALOS-AVNIR-2, EO-ASTER, IKONOS, Landsat 4 and 5 TM/ 7 ETM+ and SPOT 5 -HRV sensors for red and NIR part of spectrum. These RSR filters cover a spectral range from approximately 0.550 up to 0.950 μ m. In the literature, red and NIR bands are described for different sensors with the same name although there is a difference in the sensitivity of each band in each sensor as it is clearly shown in Figures 1 and 2.

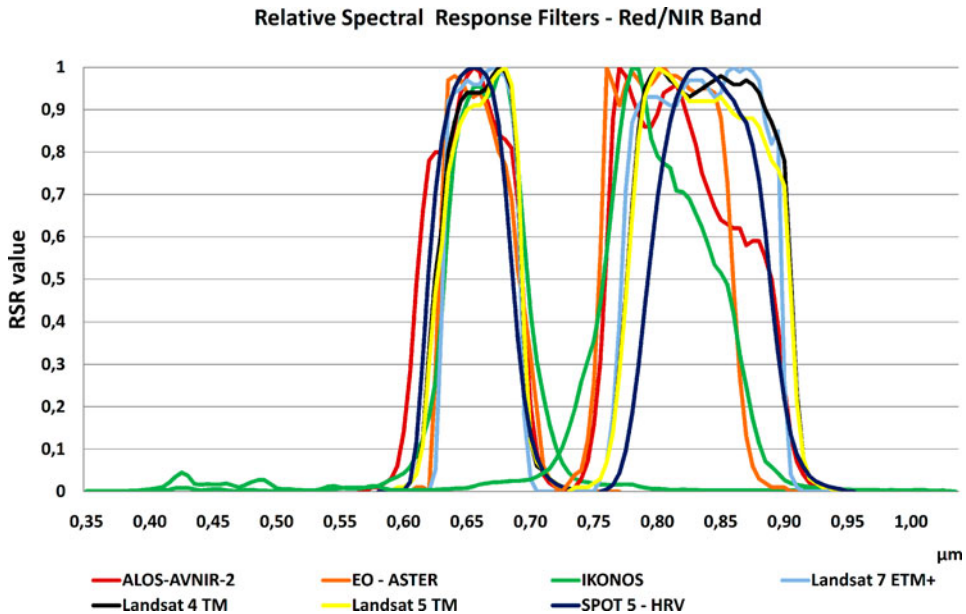


Figure 2. RSR for Red and NIR bands of the satellite sensors mentioned in this study.

3. Vegetation indices and SR index

Vegetation indices are mainly derived from reflectance data from the red and NIR bands. They operate by contrasting intense chlorophyll pigment absorption in the red against the high reflectance of leaf mesophyll in the NIR (Lasaponara and Masini 2007).

The NDVI is the one of the most widely vegetation indices used for archaeological purposes. It was first developed by Rouse *et al.* (1974) and since then it was used on several applications, including the detection of archaeological remains and the monitoring of archaeological sites. NDVI algorithm is presented in Equation (2):

$$\text{NDVI} = (p_{\text{NIR}} - p_{\text{red}}) / (p_{\text{NIR}} + p_{\text{red}}) \quad (2)$$

Where: p_{NIR} is the reflectance at NIR spectrum; p_{red} is the reflectance at red spectrum.

The SR index is also considered to be one of the commonly used vegetation indices (Tucker 1979, Sellers 1985). It provides unique information since it can be used for discriminating between soil and vegetation, such as, live green plants that reflect strongly in the NIR while absorbing in the red spectral region. On the other hand, barren surfaces (rock and soil) and water tend to reflect similarly in the red and NIR. However, SR does not give proper information when the reflected wavelengths are being affected due to topography, atmosphere or shadows (Akkartal *et al.* 2004). In addition, Chen (1996) demonstrated that the SR vegetation index was the most correlated with leaf area index. SR is defined via Equation (3).

$$\text{SR} = p_{\text{red}} / p_{\text{NIR}} \quad (3)$$

Where: p_{NIR} is the reflectance at NIR spectrum; p_{red} is the reflectance at red spectrum.

4. Overall methodology

4.1. Simulating archaeological environment

During 2010, a test field was created at Alampra village located in central Cyprus. The aim of this test field was to simulate archaeological environment for detecting architectural remains buried under ground soil. This test field was designed and developed *in situ* by the Remote Sensing Laboratory of the Cyprus University of Technology, in order to monitor spectral signatures of barley crops under different scenarios with archaeological remains. For the aims of this study a 5 m × 5 m square was used to simulate the presence of swallow depth buried remains. The test site was cultivated with barley crops according to the traditional methods of the area during 2010–2011. Local stones from the area were collected and buried approximately 25 cm beneath ground (Agapiou *et al.* 2011b). Figure 3 shows some photographs taken during the construction of the test field, the cultivation and the barley crops growing in the region.

4.2. Ground measurements

Eight typical spectral signatures of crops were examined (see Table 2) for the aims of this study. All these spectral profiles were acquired at different field campaigns at the test field. The spectral profiles were collected, using the hand-held GER1500 spectroradiometer. This instrument was recently calibrated (2010) along with the calibration spectralon panel. It has the ability to provide accurate spectral profiles covering a spectral range from 400 to 1050 nm and includes 512 different channels. Each channel covers a range of about 1.5 nm.

In detail, five different field spectroradiometric campaigns were carried out between November of 2010 and March 2011. Ground measurements were carried out between 10:00 and 14:00 (local time) in order to minimise the impact of illumination changes on the spectral responses (Milton 1987). All the measurements were taken from nadir view, from a height of 1.2 m using a 4° FOV lens under clear sky conditions (non-hazy days).



Figure 3. The test field in Alampra village during its construction, cultivation and barley growth.

Table 2. Vegetation and Soil Types experiment in this study.









No.	Description	Date of field measurement	Photo
1	Dry soil	24 November 2010	
2	Wet soil	15 December 2010	
3	Barley crops over non architectural remains (5 cm height/70% green cover)	26 December 2010	
4	Barley crops over architectural remains (5 cm height/70% green cover)	26 December 2010	
5	Barley crops over non architectural remains (40 cm height/100% green cover)	26 January 2011	

Table 2 (Continued)

No.	Description	Date of field measurement	Photo
6	Barley crops over architectural remains (40 cm height/ 100% green cover)	26 January 2011	
7	Barley crops over non architectural remains (60 cm height/ 100% green cover)	13 March 2011	
8	Barley crops over architectural remains (60 cm height/ 100% green cover)	13 March 2011	

The profile of each target (Figure 4) denotes the classic spectral characteristics of vegetation with a reflectance peak in green, minimal at blue and red part of spectrum (due to chlorophyll absorption) and high reflectance response in the NIR (due to internal leaf anatomy and scattering). On the other hand, the spectral signatures of soil show general similarities with the non-photosynthetic vegetation targets in visible and NIR parts of the spectrum (Herold *et al.* 2004).

4.3. The method

The method followed in this study for comparing spectral sensitivity of varying satellite sensors is shown in Figure 5 and is briefly described as follows:-

- Ground measurements collection;
- Scaling Up based on RSR filters and
- Evaluation of spectral signatures/vegetation indices between the different sensors.

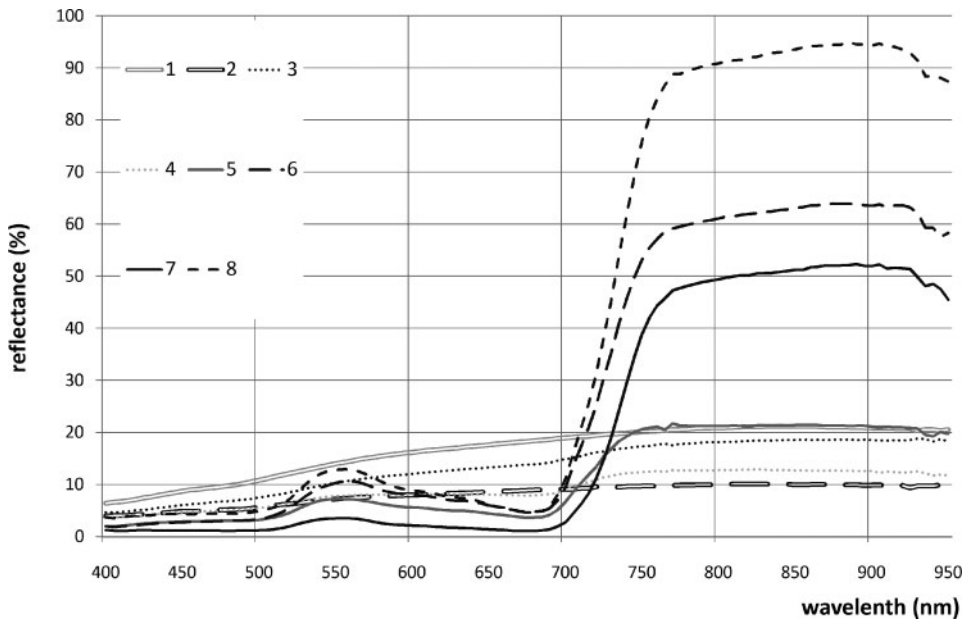


Figure 4. Spectral signatures profiles of the vegetation types and soil examined in the study (see Table 1 for description).

After the spectral signatures were acquired, red and NIR bands of different sensors (ALOS-AVNIR-2, EO-ASTER, IKONOS, Landsat 4 and 5 TM/ 7 ETM+ and SPOT 5 -HRV) were calculated using the RSR filters. Therefore, satellite images could be simulated based on ground spectral profiles. In this way, narrow wavelength bands were re-calculated in order to simulate satellite imagery bands, often used for archaeological detection.

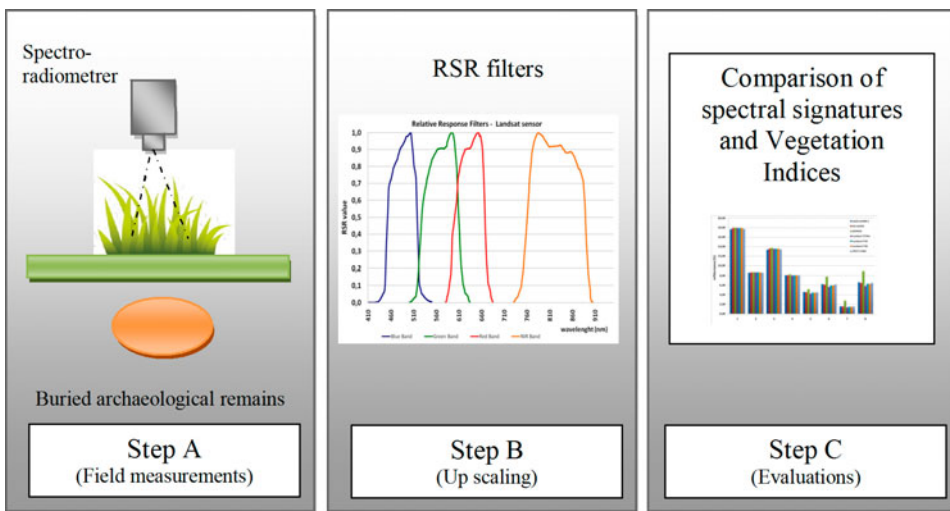


Figure 5. Methodological diagram.

The red and NIR bands of each sensor were compared in pairs of vegetation (e.g. healthy vegetation No. 3 and stress vegetation No. 4, [Table 2](#)). In this way, statistical analysis could be performed in order to identify any significant difference between the sensors. Additionally, vegetation indices (NDVI and SR) were calculated using the broadband of each sensor. Again the results were compared in pairs of vegetation.

5. Results

The comparison of the bandwidth signatures for all sensors, mentioned in this study, is presented in the first part of this chapter. The second part is focused on the evaluation of the sensors regarding vegetation indices (NDVI, SR).

5.1. Bandwidth signatures

Using RSR filters for the red and NIR bands, the reflectance response of each different type of vegetation and soil for the seven different satellite sensors (ALOS-AVNIR-2, EO-ASTER, IKONOS, Landsat 4 and 5 TM/ 7 ETM+ and SPOT 5 -HRV). [Figures 6](#) and [7](#) shows the absolute reflectance for each one of the targets. Minor differences were observed between the various sensors. Substantial differences were recorded for IKONOS reflectance.

Specifically, for soil targets (both dry and wet), the reflectance response is approximately the same for all sensors and the relative difference is calculated to be between 0.8% and 1.3%. It is interesting to note that, wet soil reflectance deviation is smaller than that of the dry soil. In addition, when barley starts to grow (targets 3 and 4)

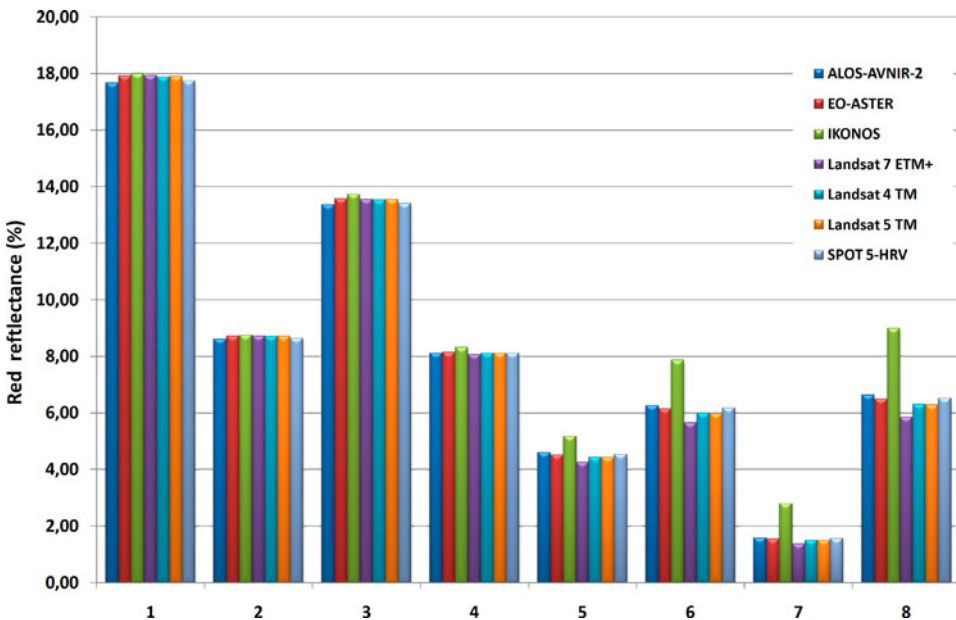


Figure 6. Red band reflectance for all sensors and spectral signatures (X-axis, see [Table 2](#)) mentioned in this study.

the reflectance values remain the same for all sensors except of a small difference occurred in the case of IKONOS sensor. This difference tends to get greater as barley grows further (targets 5–6) and is maximised when the barley crops approach the 60 cm height (targets 7–8). However, in all different cases of vegetation cover, IKONOS sensor tends to record lower reflectance values for the NIR band (1–8%) and higher reflectance values for the red band (0.5–3%), compared to Landsat ETM+ and other sensors.

Red reflectance (Figure 6) and NIR reflectance (Figure 7) for barley crops, over non buried architectural remains, (targets 3; 5 and 7) tend to get lower when barley starts to grow. Similarly, this is also observed for crops over the architectural remains (targets 4; 6 and 8).

Figures 8 and 9 indicate the relative difference of these reflectance values compared to those of Landsat ETM+ sensor. The Landsat ETM+ sensor was chosen to be as the reference sensor. IKONOS sensor tends to give higher reflectance values (up to 3%) for barley crops (targets 3–8) in the red spectrum and lower reflectance values (up to 8%) in the NIR spectrum. All other sensors tend to give similar results, which were calculated <1% for both red and NIR bands. The significant difference of sensitivity which is recorded for IKONOS compared to the other sensors is related with the spectral resolution of the sensor. It is obvious therefore, that small differences in the spectral resolution of the sensor (as shown in Table 1 and Figure 1), can produce a noteworthy change to the recorded reflectance of the sensor. Based on these remarks, it is also significant to estimate the spectral sensitivity and the spectral differences of all sensors mentioned in the study regarding vegetation indices.

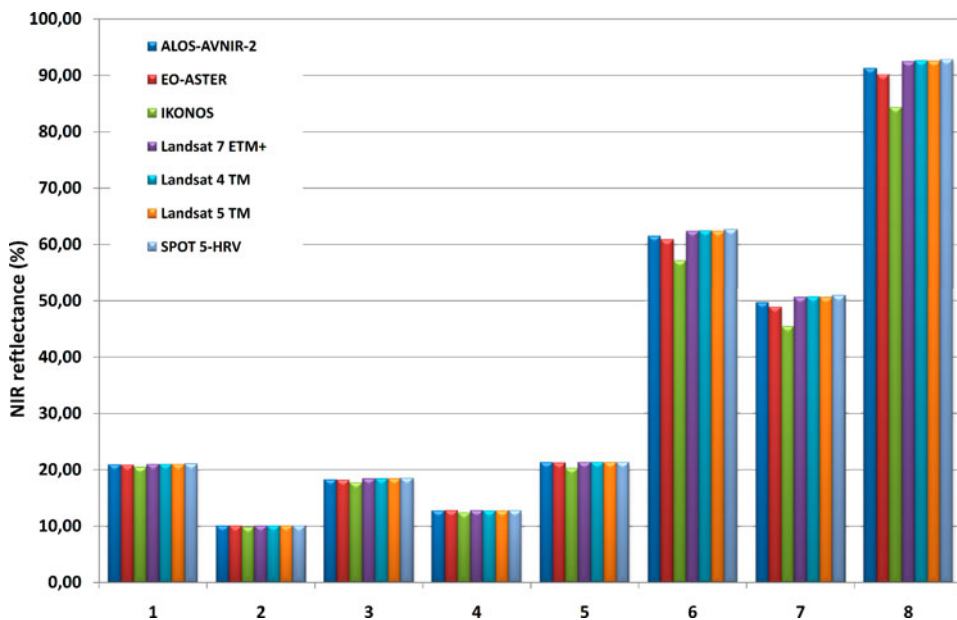


Figure 7. NIR band reflectance for all sensors and spectral signatures (X-axis, see Table 2) mentioned in this study.

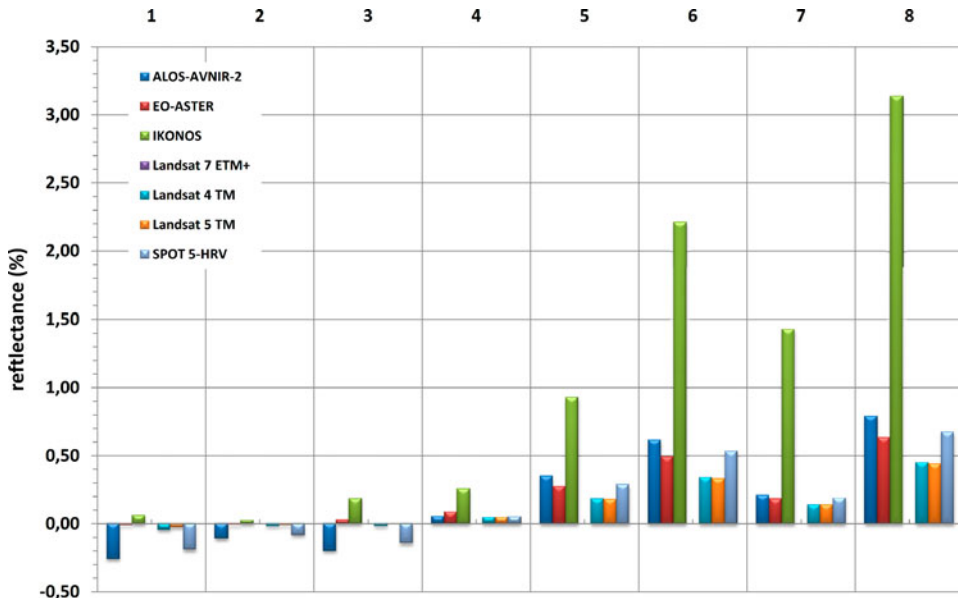


Figure 8. Relative comparison of Red band reflectance.

5.2. Vegetation indices profiles

Figures 10 and 11 show the NDVI and SR values for all the sensors and all the targets, respectively. NDVI and SR are expected to be higher for healthy vegetation, since plants absorb solar radiation in the photosynthetically active spectral region, which plants use as a source of energy in the process of photosynthesis. Table 3 gives the

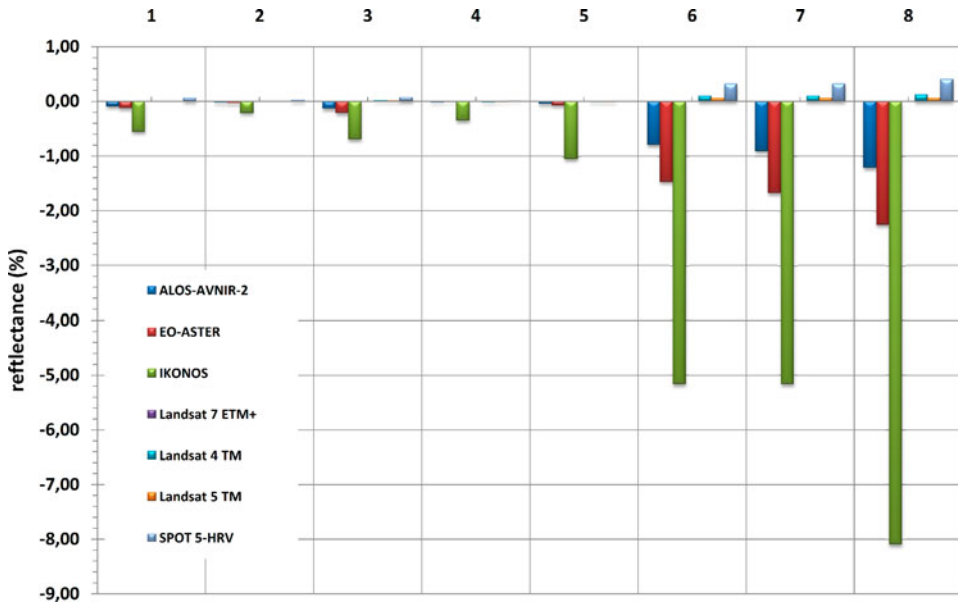


Figure 9. Relative comparison of NIR band reflectance.

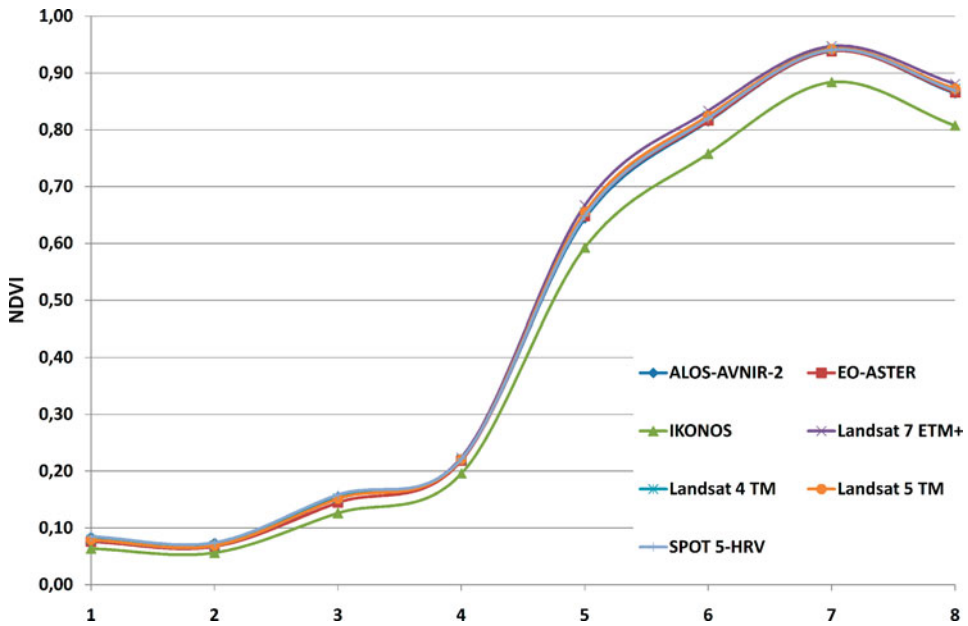


Figure 10. NDVI as calculated for the satellite sensors for all spectral signatures.

absolute value of the NDVI, while Table 4 gives the absolute values of the SR index. Concerning these statistics, targets 1–4 do not show any significant difference between the sensors. In contrast, IKONOS values seem to give steady lower response. However, for the more vegetated targets 5–8, IKONOS sensor continues to give smaller NDVI

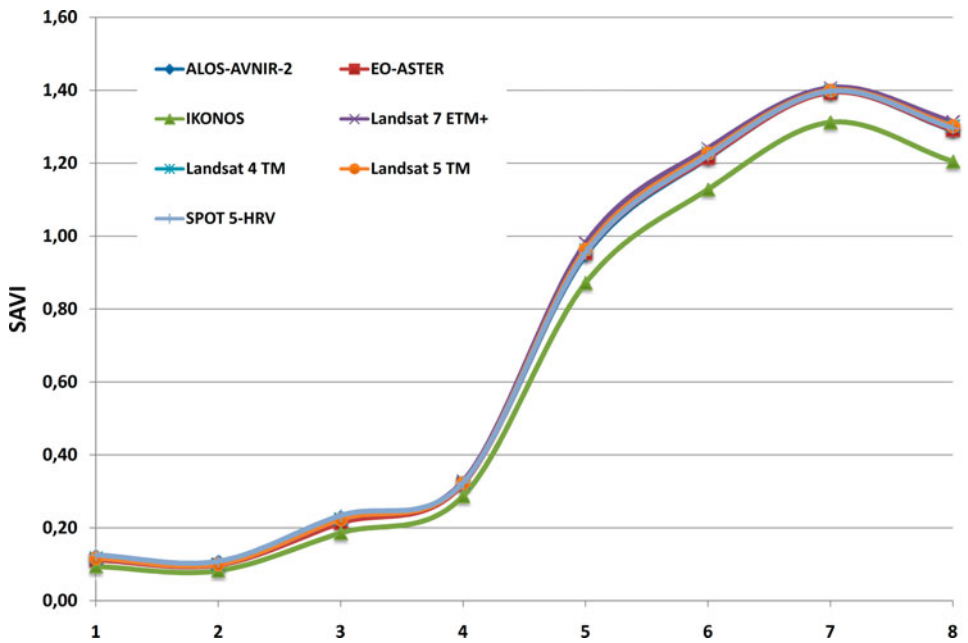


Figure 11. SR as calculated for the satellite sensors for all spectral signatures.

Table 3. NDVI values as calculated for all sensors and spectral signatures.

Sensor	NDVI values for all vegetation and soil types							
	1	2	3	4	5	6	7	8
ALOS-AVNIR-2	0.08	0.07	0.16	0.22	0.64	0.82	0.94	0.86
EO-ASTER	0.08	0.07	0.14	0.22	0.65	0.82	0.94	0.87
IKONOS	0.06	0.06	0.13	0.20	0.59	0.76	0.88	0.81
Landsat 7 ETM+	0.08	0.07	0.15	0.22	0.67	0.83	0.95	0.88
Landsat 4 TM	0.08	0.07	0.15	0.22	0.66	0.82	0.94	0.87
Landsat 5 TM	0.08	0.07	0.15	0.22	0.66	0.82	0.94	0.87
SPOT 5-HRV	0.09	0.07	0.16	0.22	0.65	0.82	0.94	0.87

and SR values compared to the other satellites. Quantitatively, the difference of NDVI values for IKONOS is approximately 0.06–0.07 (6–7%) less than other sensors.

Moreover, Landsat sensors (TM/ETM+) seem to give very similar results with a small variation (± 0.01 NDVI or 1% difference) and therefore one can argue that if pre-processing steps are performed for archive and new overpass satellite Landsat images then these images can be used as a standard for direct comparison of vegetation using the NDVI algorithm. However, for SR index the relative values between different sensors can be very high since SR index is not normalised as NDVI. Moreover, considering SR index, it is important to mention the substantial difference that is recorded between the healthy and stress measurements of barley crops during spring period. This interval in the values highlights the potential of the specific index in archaeological prospection studies, in the case of buried remains, under barley crops, because of the corresponding contrast in the values between the area of archaeological context and the surroundings. This can also be stated for NDVI, but in a much smaller grade concerning barley crops of 40 cm height (period of January).

Percentage difference between NDVI values for targets 3–4; 5–6 and 7–8 was also examined. Larger variation between archaeological and in non archaeological areas can result in better interpretations of images for the detection and identification of crops marks. As it was found, IKONOS shows the highest difference of the NDVI value for all pair of crops. This difference tends to get smaller while the crop is growing. However, for crops not taller than 40 cm, the NDVI difference can be reached up to 8% (ALOS-AVNIR-2). Similarly, a significant difference is recorded for the SR index (15% higher difference for targets 7–8) as well.

Table 4. SR values as calculated for all sensors and spectral signatures.

Sensor	SR values for all vegetation and soil types							
	1	2	3	4	5	6	7	8
ALOS-AVNIR-2	1.18	1.16	1.37	1.57	4.62	9.82	31.52	13.75
EO-ASTER	1.16	1.14	1.34	1.56	4.69	9.90	31.61	13.92
IKONOS	1.14	1.12	1.29	1.49	3.91	7.27	16.24	9.39
Landsat 7 ETM+	1.17	1.15	1.36	1.58	5.01	11.03	37.04	15.82
Landsat 4 TM	1.17	1.15	1.36	1.57	4.80	10.42	33.70	14.71
Landsat 5 TM	1.17	1.15	1.36	1.57	4.80	10.43	33.67	14.72
SPOT 5-HRV	1.19	1.16	1.38	1.57	4.69	10.13	32.72	14.25

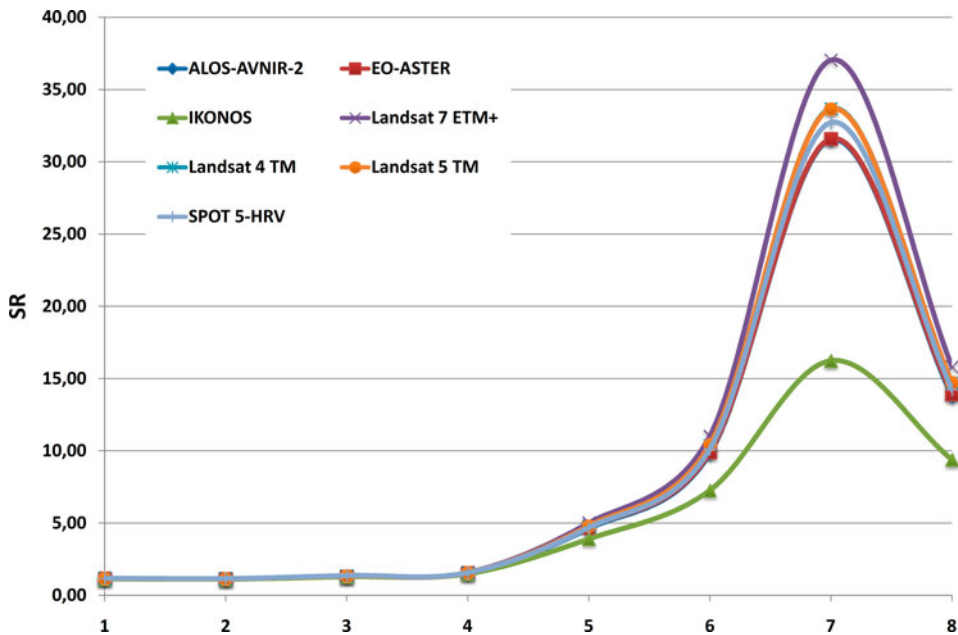


Figure 12. Relative NDVI values of all sensors relative to Landsat ETM+.

Figure 12 and Table 5 present the relative NDVI values for the satellite sensors compared to the NDVI values of Landsat ETM+. Near to zero relative values of NDVI are expected if the sensitivity of each sensor is similar to the sensitivity of Landsat for NDVI. As it is shown in Figure 12, a range of relative difference from -0.05 to 0.08 is recorded for ALOS-AVNIR-2, EO-ASTER, Landsat Landsat 4 and 5 TM and SPOT 5 -HRV. The relative difference of IKONOS is greater and ranges from -0.05 to -0.15 for vegetation targets and -0.15 to -0.25 for soil targets.

Furthermore, a second polynomial best fit curve was used for correlation between these values. From the results, a strong correlation is suggested for all sensors compared to Landsat ETM+ (over 78%) except that of EO-ASTER images (50%). In addition, relative NDVI values of IKONOS sensor compared to the Landsat 7 are high as 25% for non-fully vegetated targets (1-4) and approximately 10% for the vegetated targets (5-8).

Figure 13 and Table 6 provide the relative SR values for the satellite sensors compared to those of Landsat ETM+. As shown in Figure 13, a small relative difference is recorded for the majority of the targets and the sensors. However, concerning IKONOS, a substantial relative difference that ranges from 20% to 70% is

Table 5. Second order polynomial best fit curve to relative NDVI difference.

Sensor	Equation (2nd polynomial order best fit)	R ²
ALOS-AVNIR-2	$y = 39.49x^2 - 46.97x + 8.908$	0.926
EO-ASTER	$y = 7.997x^2 - 6.117x - 2.449$	0.499
IKONOS	$y = -11.41x^2 + 26.44x - 23.37$	0.909
Landsat 4 TM	$y = 14.55x^2 - 16.65x + 2.449$	0.884
Landsat 5 TM	$y = 7.934x^2 - 9.347x + 1.202$	0.787
SPOT 5-HRV	$y = 39.79x^2 - 48.40x + 10.40$	0.911

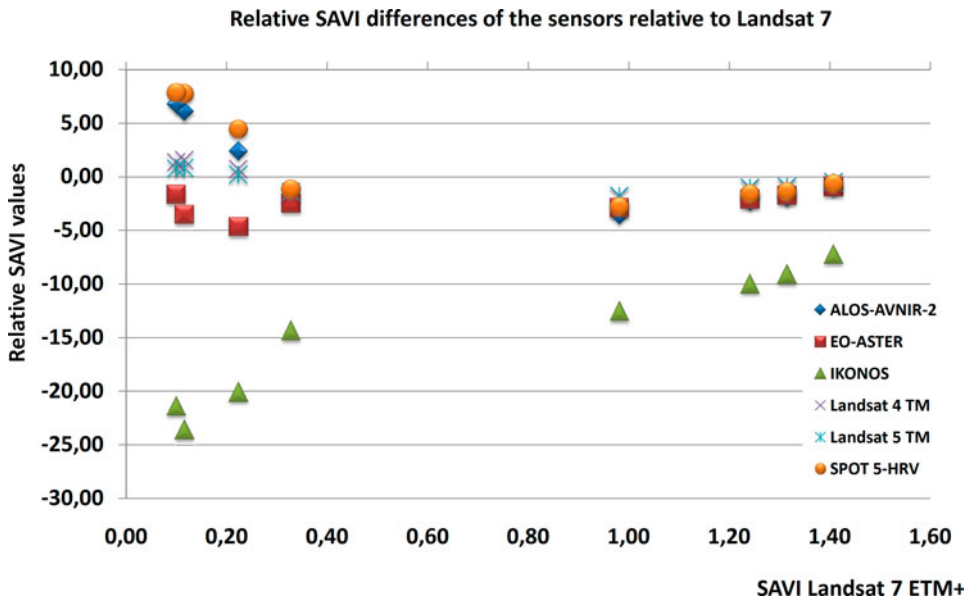


Figure 13. Relative SR values of all sensors relative to Landsat ETM+.

Table 6. Second order polynomial best fit curve to relative SR difference.

Sensor	Equation (2nd polynomial order best fit)	R^2
ALOS-AVNIR-2	$y = 0.029x^2 - 1.632x + 2.071$	0.968
EO-ASTER	$y = 0.022x^2 - 1.303x + 0.587$	0.988
IKONOS	$y = 0.051x^2 - 5.393x + 2.024$	0.998
Landsat 4 TM	$y = 0.012x^2 - 0.75x + 0.689$	0.967
Landsat 5 TM	$y = 0.011x^2 - 0.724x + 0.584$	0.971
SPOT 5-HRV	$y = 0.022x^2 - 1.245x + 1.942$	0.950

mainly recorded for vegetated areas. Similar to NDVI case, a second polynomial best fit curve was used in order to correlate these values. The results indicated a strong correlation between all the sensors compared to Landsat ETM+ (over 90%) for the SR index.

6. Conclusions

In this study the sensitivity of seven common satellite sensors, used for archaeological prospection studies, was tested and validated. The measurements were acquired over a test field which was specially constructed to simulate an archaeological environment. Moreover, the measurements were acquired in different periods of barley's crop's phenological cycle. All the measurements were re-calculated to broadband satellite sensors measurements using RSR filters. The results denoted that the vast majority of the sensors compared with each other seem to have approximately the same accuracy and sensitivity. However, in certain cases of barley crops, a substantial difference

between archaeological area and non archaeological area values in red and NIR band of spectrum is recorded, which facilitates the detection of shallow sub-surface remains. Further, the IKONOS sensor seems to be more sensitive to vegetation (comparing stress and non stress vegetation), in a range of approximately 1–8% compared to the other sensors. The difference exceeds the relative uncertainties of calibration that ranges within 5% for satellite sensors according to relevant literature. Additionally, in this study vegetation indices such as SR and NDVI were used to illustrate the potential of each sensor for detecting sub-surface archaeological remains. Although the SR index is considered to be a simple and quite common applied vegetation index, the results demonstrated the utilisation of SR index as an auxiliary methodology to main archaeological research for detecting buried remains. The substantial difference between the SR values of the stress and non stress pixels highlights the potential of the specific index to contribute to the delineation of shallow sub-surface remains and produce a well defined contrast signal to the surroundings patterns. Additionally, an intrinsic difference in the percentage of sensitivity of NDVI and SR values of IKONOS sensor was observed compared to the other sensors. This fact suggests that further investigation of the potential of these indices, extracted from satellites with similar characteristics as IKONOS, an essential task for archaeological research. This difference of IKONOS might be a result of the spectral resolution of the sensor which is quite different from all the other sensors compared in this study. These small differences in the spectral resolution of the sensor can provide results with a noteworthy change to the recorded reflectance of the sensor.

Moreover, the study revealed the great utility of hand held spectroradiometer to archaeological prospection in a two fold way. Firstly, the ground measurements can be easily compared using RSR filters with any kind of satellite measurements, in order to validate their results and constitute an integrated remote sensing approach in archaeological research. Secondly, the great range of spectroradiometric data offers always the chance to detect a vegetation anomaly related to bury archaeological remains. Finally, the whole methodology can be used as a road map for any potential users of different satellite imagery for archaeological purposes. Specifically, the researchers may have the ability to evaluate the satellites spectral sensitivity before proceeding to the acquisition of image either in known archaeological fields or even in simulated test fields (as shown in this study) based on ground spectroradiometric campaigns. The authors will continue to carry out further field measurements over other crop types in order to evaluate the overall sensitivity of multispectral/hyperspectral sensors.

Acknowledgements

These results are part of the Ph.D. thesis of Mr. Athos Agapiou. The authors would like to express their appreciation to the Alexander Onassis Foundation for funding the Ph.D. study. Thanks are given to the Remote Sensing Laboratory of the Department of Civil Engineering & Geomatics at the Cyprus University of Technology for the support (<http://www.cut.ac.cy/>). Also thanks are given to Mr Costas Tsiartas for editing the article.

References

- Agapiou, A. *et al.*, 2012. Observatory validation of Neolithic tells (“Magoules”) in the Thessalian plain, central Greece, using hyperspectral spectroradiometric data. *Journal of Archaeological Science*, 39, 1499–1512.

- Agapiou, A. *et al.*, 2011a. The importance of accounting for atmospheric effects in the application of NDVI and interpretation of satellite imagery supporting archaeological research: the case studies of Palaepaphos and Nea Paphos sites in Cyprus. *Remote Sensing*, 3 (12), 2605–2629.
- Agapiou, A. *et al.*, 2011b. Exploring ground spectroscopy for the detection of sub-surfaces architectural remains: the methodological context. In *Proceedings XVI Congress of the UISPP (International Union for Prehistoric and Protohistoric Sciences)*, 4–10 September, Florianopolis, Brazil (in press).
- Agapiou, A. and Hadjimitsis, D.G. 2011. Vegetation indices and field spectroradiometric measurements for validation of buried architectural remains: verification under area surveyed with geophysical campaigns. *Journal of Applied Remote Sensing*, 5, 05355. DOI:10.1117/1.3645590
- Agapiou, A., *et al.*, 2010. Hyperspectral ground truth data for the detection of buried architectural remains. *Lecture Notes of Computer Science*, 6436, 318–331.
- Akkartal, A., Türüdü, O., and Erbek, F.S. 2004. Analysis of changes in vegetation biomass using multisensor satellite data. *Proceedings of the ISPRS Congress-Youth Forum*, XXXV, 181–185.
- Alexakis, A., *et al.*, 2011. Integrated GIS, remote sensing and geomorphologic approaches for the reconstruction of the landscape habitation of Thessaly during the neolithic period. *Journal of Archaeological Science*, 38, 89–100.
- Alexakis, D., *et al.*, 2009. Detection of neolithic settlements in Thessaly (Greece) through multispectral and hyperspectral satellite imagery. *Sensors*, 9, 1167–1187.
- Altaweel, M., 2005. The use of ASTER satellite imagery in archaeological contexts. *Archaeological Prospection*, 12, 151–166.
- Beck, A., 2007. Archaeological site detection: the importance of contrast. In *Proceedings of the Annual Conference of the Remote Sensing and Photogrammetry Society*, 11–14 September, Newcastle Upon Tyne, Newcastle University.
- Bewley, R.H., 2003. Aerial Survey for Archaeology. *The Photogrammetric Record*, 18 (104), 273–292.
- Campbell, J.B. 2002. *Introduction to remote sensing*. London and New York: Guilford Press.
- Chander, G., Markham, L.B., and Helder, L.D., 2009. Summary of current radiometric calibration coefficients for Landsat MSS, TM, ETM+, and EO-1 ALI sensors. *Remote Sensing of Environment*, 113, 893–903.
- Chen, J., 1996. Evaluation of vegetation indices and modified simple ratio for boreal applications. *Canadian Journal of Remote Sensing*, 22, 229–242.
- Ciminale, M. *et al.*, 2009. A multiscale approach for reconstructing archaeological landscapes: applications in Northern Apulia (Italy). *Archaeological Prospection*, 16, 143–153. DOI: 10.1002/arp.356
- Clark, C.D., Garrod, S.M., and Pearson, M.P., 1998. Landscape archaeology and remote sensing in southern Madagascar. *International Journal of Remote Sensing*, 19 (8), 1461–1477.
- Curran, P.J. and Williamson, H.D., 1986. Sample size for ground and remotely sensed data. *Remote Sensing of Environment*, 20, 31–41.
- Hadjimitsis, D.G. *et al.*, 2011. Exploring natural and anthropogenic risk for cultural heritage in Cyprus using remote sensing and GIS. *International Journal of Digital Earth*. DOI:10.1080/17538947.2011.602119
- Hadjimitsis, D.G. *et al.*, 2009. Multi-temporal study of archaeological sites in Cyprus using atmospheric corrected satellite remotely sensed data. *International Journal of Architectural Computing*, 7 (1), 121–138 (18). DOI: 10.1260/147807709788549376
- Herold, M., *et al.*, 2004. Spectrometry for urban area remote sensing: development and analysis of a spectral library from 350 to 2400 nm. *Remote Sensing of Environment*, 91 (3–4), 30, 304–319. ISSN 0034-4257, DOI: 10.1016/j.rse.2004.02.013
- Jarvis, P.G., 1995. Scaling processes and problems. *Plant Cell & Environment*, 18, 1079–1089.
- Jonson, K.J., 2006. *Remote sensing in archaeology. An explicitly North America perspective*. Tuscaloosa, AL: The University of Alabama Press.
- Laet, V., Paulissen, E., and Waelkens, M., 2007. Methods for the extraction of archaeological features from very high-resolution Ikonos-2 remote sensing imagery, Hisar (southwest Turkey). *Journal of Archaeological Science*, 34, 830–841.

- Lasaponara, R. and Masini, N., 2001. Satellite remote sensing in archaeology: past, present and future perspectives. *Journal of Archaeological Science*, 38 (9), 995–2002. DOI:[10.1016/j.jas.2011.02.002](https://doi.org/10.1016/j.jas.2011.02.002)
- Lasaponara, R. and Masini, N., 2005. QuickBird-based analysis for the spatial characterization of archaeological sites: case study of the Monte Serico Medioeval village. *Geophysical Research Letter*, 32 (12), L12313.
- Lasaponara, R. and Masini, N., 2006. Identification of archaeological buried remains based on Normalized Difference Vegetation Index (NDVI) from Quickbird satellite data. *IEEE Geoscience and Remote Sensing Letters*, 3 (3), 325–328.
- Lasaponara, R. and Masini, N., 2007. Detection of archaeological crop marks by using satellite QuickBird multispectral imagery. *Journal of Archaeological Science*, 34, 214–221.
- Lillesand, M., Kiefer, T., and Chipman, J.W., 2004. *Remote sensing and image interpretation*. New York, NY: Wiley International Edition.
- Malenovský, Z., *et al.*, 2007. Scaling dimensions in spectroscopy of soil and vegetation. *International Journal of Applied Earth Observation and Geoinformation*, 9 (2), 137–164.
- Marceau, J.D., *et al.*, 1994. Remote sensing and the measurement of geographical entities in a forested environment. 2. The optimal spatial resolution. *Remote Sensing of Environment*, 49 (2), 105–117.
- Markham, B.L. and Barker, J.L., 1985. Spectral characterization of the LANDSAT Thematic Mapper sensors. *International Journal of Remote Sensing*, 6 (5), 697–716.
- Markham, B.L., *et al.*, 1997. Landsat-7 enhanced Thematic Mapper plus radiometric calibration. *Canadian Journal of Remote Sensing*, 23 (4), 318–332.
- Masini, N. and Lasaponara, R., 2007. Investigating the spectral capability of QuickBird data to detect archaeological remains buried under vegetated and not vegetated areas. *Journal of Cultural Heritage*, 8, 53–60.
- Mills, J. and Palmer, R., 2007. *Populating clay landscapes*. Stroud, UK: Tempus.
- Milton, J., 1987. Principles of field spectroscopy. *Remote Sensing of Environment*, 8 (12), 1807–1827.
- Milton, E.J. and Rollin, E.M., 2006. Estimating the irradiance spectrum from measurements in a limited number of spectral bands. *Remote Sensing of Environment*, 100 (3), 348–355. DOI:[10.1016/j.rse.2005.10.016](https://doi.org/10.1016/j.rse.2005.10.016)
- Milton, E.J., *et al.*, 2009. Progress in field spectroscopy. *Remote Sensing of Environment*, 113, 92–109.
- Papadavid, G. *et al.*, 2011. Mapping potato crop height and leaf area index through vegetation indices using remote sensing in Cyprus. *Journal of Applied Remote Sensing*, 5, 053526. DOI:[10.1117/1.3596388](https://doi.org/10.1117/1.3596388)
- Parcak, S.H., 2009. *Satellite remote sensing for archaeology*. London and New York: Routledge Taylor and Francis Group.
- Peddle, D.R., *et al.*, 2001. Reflectance processing of remote sensing spectroradiometer data. *Computers & Geosciences*, 27, 203–213.
- Riley, D.N., 1979. Factors in the development of crop marks. *Aerial Archaeology*, 4, 28–32.
- Rouse, J.W. *et al.*, 1974. *Monitoring the vernal advancements and retrogradation (greenwave effect) of nature vegetation, NASA/GSFC Final Report*. Greenbelt, MD: Texas A & M University, Remote Sensing Center College Station.
- Rowlands, A. and Sarris, A., 2007. Detection of exposed and subsurface archaeological remains using multi-sensor remote sensing. *Journal of Archaeological Science*, 34, 795–803.
- Sarris, A. and Jones, R., 2000. Geophysical and related techniques applied to archaeological survey in the Mediterranean: a review. *Journal of Mediterranean Archaeology*, 13 (1), 3–75.
- Sellers, P.J., 1985. Canopy reflectance, photosynthesis and transpiration. *International Journal of Remote Sensing*, 6, 1335–1372.
- Sharpe, L., 2004. *Geophysical, geochemical and arable crop responses to archaeological sites in the Upper Clyde Valley, Scotland*. Thesis (PhD). University of Glasgow.
- Stanjek, H. and Fabinder, J.W.E., 1995. Soil aspects affecting archaeological details in aerial photographs. *Archaeological Prospection*, 2 (1), 91–101.
- Teillet, P.M., *et al.*, 2007. Impacts of spectral band difference effects on radiometric cross-calibration between satellite sensors in the solar-reflective spectral domain. *Remote Sensing of Environment*, 110 (3), 393–409. ISSN 0034-4257, DOI: [10.1016/j.rse.2007.03.00](https://doi.org/10.1016/j.rse.2007.03.00)

- Tran, D.-B.T. *et al.*, 2011. Optimizing spatial resolution of imagery for urban form detection—the cases of France and Vietnam. *Remote Sensing*, 3, 2128–2147. DOI:[10.3390/rs3102128](https://doi.org/10.3390/rs3102128)
- Tripathi, A., 2000. *Remote sensing and archaeology*. New Delhi: Sundeep Prakashan.
- Trishchenko, P.A., 2009. Effects of spectral response function on surface reflectance and NDVI measured with moderate resolution satellite sensors: extension to AVHRR NOAA-17, 18 and METOP-A. *Remote Sensing of Environment*, 113 (2), 335–341. ISSN 0034-4257, DOI: [10.1016/j.rse.2008.10.002](https://doi.org/10.1016/j.rse.2008.10.002)
- Trishchenko, P.A., Cihlar, J., and Zhanqing, L., 2002. Effects of spectral response function on surface reflectance and NDVI measured with moderate resolution satellite sensors. *Remote Sensing of Environment*, 81 (1), 1–18. ISSN 0034-4257, DOI: [10.1016/S0034-4257\(01\)00328-5](https://doi.org/10.1016/S0034-4257(01)00328-5)
- Tucker, C.J., 1979. Red and photographic infrared linear combinations for monitoring vegetation. *Remote Sensing of Environment*, 8 (2), 127–150.
- Winton, H. and Horne, P. 2010. National archives for national survey programmes: NMP and the English heritage aerial photograph collection. In *Landscapes through the Lens*. Aerial Photographs and Historic Environment. Aerial Archaeology Research Group No. 2, 7–18.
- Wu, H. and Liang Li, Z. 2009. Scale issues in remote sensing: a review on analysis, processing and modeling. *Sensors*, 9, 1768–1793. DOI:[10.3390/s90301768](https://doi.org/10.3390/s90301768)
- Wu, X., Sullivan, T.J., and Heidinger, K.A., 2010. Operational calibration of the advanced very high resolution radiometer (AVHRR) visible and near-infrared channels. *Canadian Journal of Remote Sensing*, 36 (5), 602–616.